CUMULATIVE FATIGUE DISBOND OF ADHESIVE JOINTS AND ITS DETECTION USING THERMAL WAVE IMAGING

H. Aglan, S. Shroff and Z. Abdo
Department of Mechanical Engineering
Tuskegee University
Tuskegee, Al 36088

T. Ahmed, L. Wang, L.D. Favro and R.L. Thomas
Institute for Manufacturing Research
Wayne State University
Detroit, MI 48201

INTRODUCTION

Adhesively bonded structures have found increased acceptance in both military and commercial aircraft. Reliability of these aircraft structures is of paramount importance. This issue is especially important for aging aircraft, which are very often in service beyond their stipulated lifetime. Joints are exposed to various combinations of cumulative mechanical fatigue, thermal fatigue and environmental conditions. In addition, voids inherent in the adhesive joint cause sites of stress concentration and coalesce to form disbonds when the joints are loaded. Simultaneous presence of these disbonds in the same structural element will result in a loss of its load bearing strength. Moisture can also attack the primary bonds between the substrate and the adhesive decreasing the joint's interfacial strength. Periodic cycling and environmental factors lead to disbond propagation and premature failure of the joints. The effect of cumulative cycling on disbonding and its propagation in adhesive joints is an important subject, which has been the focus of this study.

Disbond detection in adhesive joints and its analyses after periodic cycling is vital to determine the integrity of adhesively bonded structures. Numerous methods have been employed to measure the integrity of adhesively bonded joints [1-5]. NDE techniques have also been applied to evaluate the adhesive-adherend interface [6-10]. The effect of adhesive type and substrate thickness on the capability of various NDE techniques to detect fatigue disbonds has been studied [11]. It should be emphasized however, that none of the currently used NDE techniques can characterize the strength of a joint. Therefore, these techniques are more useful if they can be linked to parameters controlling the fracture process. The strength of an adhesive bond is predominantly dependent on the quality of the interlayer between the adhesive and the adherend. Since the thickness of this layer is generally on the order of 1 μm, detection of this region is important before and during service [12].

In the present work, multiple identical joints (without and with rivet holes) fabricated using aircraft grade aluminum and structural adhesive were cycled to various levels of their lifetime. Before cycling and after every round of cycling, the joints were scanned using thermal wave imaging and later correlated with microscopic observations taken during the fatigue cycling.

MATERIALS AND EXPERIMENTAL PROCEDURE

Multiple identical substrates were machined to 140 x 76.2 mm^2 from 1 mm thick aluminum 2024-T3 sheets. The substrates were milled to a half dogbone shape with a bondline width of 50.8 mm. The half dogbone substrates were degreased with a 50/50 isopropyl alcohol/water mixture. Then, 3M scrim cloth structural adhesive prepreg (AF-163-2K) of about 0.25 mm nominal thickness was applied on one of the substrates. The other mating surface was then overlapped to have a bonded area of 25.4 mm long and 50.8 mm wide, as shown in Figure 1. This bonded area was chosen after preliminary tests to ensure that the failure load of the joint was well below the load required to cause tensile failure of the substrate. The specimens were heat cured at a temperature of 121°C and pressure of 3.45 MPa for 1 hour and then allowed to cool slowly to room temperature. Two rivet holes of 4 mm diameter, were drilled 25.4 mm center to center, in half of the joints to resemble an actual rivet hole geometry of a fuselage part [13]. The adhesive thickness was measured at different points to ensure uniform bondline thickness.

A set of six specimens (three without and three with rivet holes) were tested in tension-tension fatigue mode. Thermal wave image scans were performed on these specimens before testing. The specimens were then fatigued to approximately 25% of the average corresponding lifetime to failure obtained from specimens previously tested to complete failure. A second round of thermal images were taken after the first round of fatigue testing. This procedure was repeated two more times. The fatigue tests were conducted on an 100 kN MTS 810 servo hydraulic machine between 890-8896 N at a mean load of 4893 N and a frequency of 3 Hz. During the cycling of the specimens, the number of cycles, the hysterisis loop and the crack lengths measured from the side of the specimen were recorded periodically.

THERMAL WAVE IMAGING

Thermal wave imaging of adhesive bond specimens was performed using Wayne State University's thermal wave imaging system [14], consisting of a pulsed heat source, typiclly high-power photographic flash lamps, an IR (infrared) video camera, and image processing hardware and software, controlled by a personal computer. A schematic diagram of the experimental setup is shown in Fig. 2. The heat source consists of a bank of six 6.4 kJ, 2 ms pulse flash lamps, fired simultaneously. The energy from these lamps is absorbed at the sample surface which changes the surface temperature distribution. This modification occurs with a delay which is characteristic of the time of flight of the pulse down to the interface and back in as much the same way an acoustic echo would return after a time delay. The returns of the thermal wave echoes are monitored by means of the IR video camera, which follows the time-dependent surface distribution of the IR emission from the surface. Only a single flash is required for the gated image processing and the intention is to capture the returning thermal wave echoes from any subsurface defects of adhesive disbonds when their contrast with the background is near its maximum value.

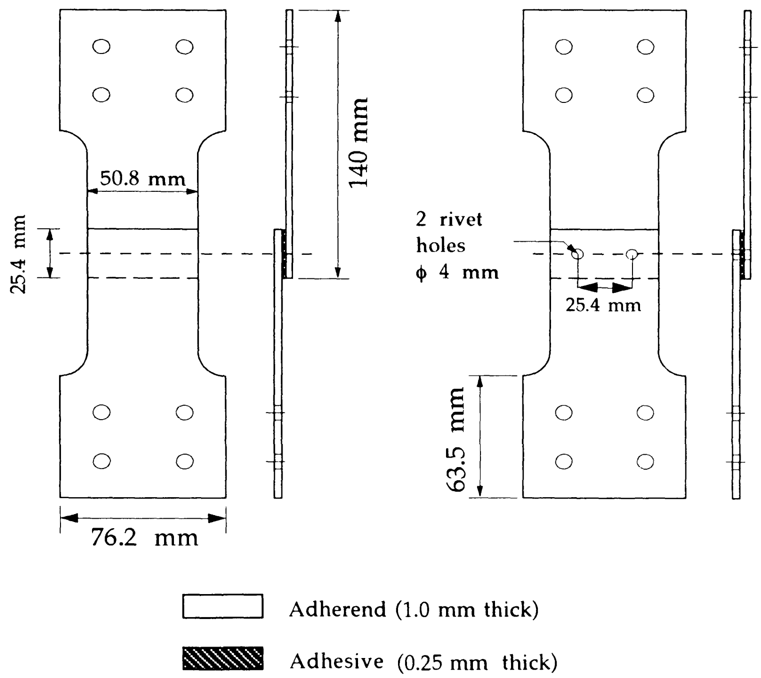

Figure 1. Specimen geometry.

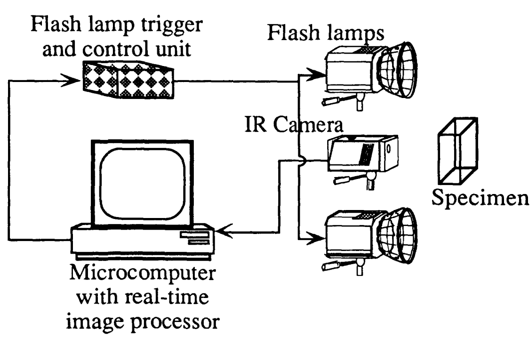

Figure 2. Experimental setup for thermal wave imaging.

RESULTS AND DISCUSSION

The disbond lengths were measured from the edges of the specimens using a traveling optical microscope and recorded with a video camera. A straight line was then joined to the opposite sides of the disbond and the area was calculated assuming a trapezoid shaped disbond.

The disbond area versus the corresponding number of cycles for specimens without and with rivet holes were taken as criterion for studying the effect of cumulative damage on adhesive bonds. It should be noted that, the data shown in Figures 3 and 6, is an average of three specimens for each particular case. Figure 3 compares the microscopically recorded area of the fatigue to failure data with the cumulative fatigue data. It is observed that, the interfacial (measurable) disbond is about 60% of the total bonded area in both cases. The joint's lifetime however, is decreased by about 33% and 24% for joints without and with rivet holes respectively, as a result of the cumulative fatigue loading. It can be seen from figures 3 a and b that the fatigue to failure and cumulative data are identical upto approximately 25% of the fatigue to failure lifetime. Thereafter the relationships between the disbond area and the number of cycles for the cumulative fatigued specimens rises more steeper. This is true for specimens without and with rivet holes. This difference probably can be attributed to environmental aging of the interfacial bonds, since humidity can attack the interfacial surface, which was disbonded during the first round of cumulative fatigue testing. This would cause the disbond rate to increase.

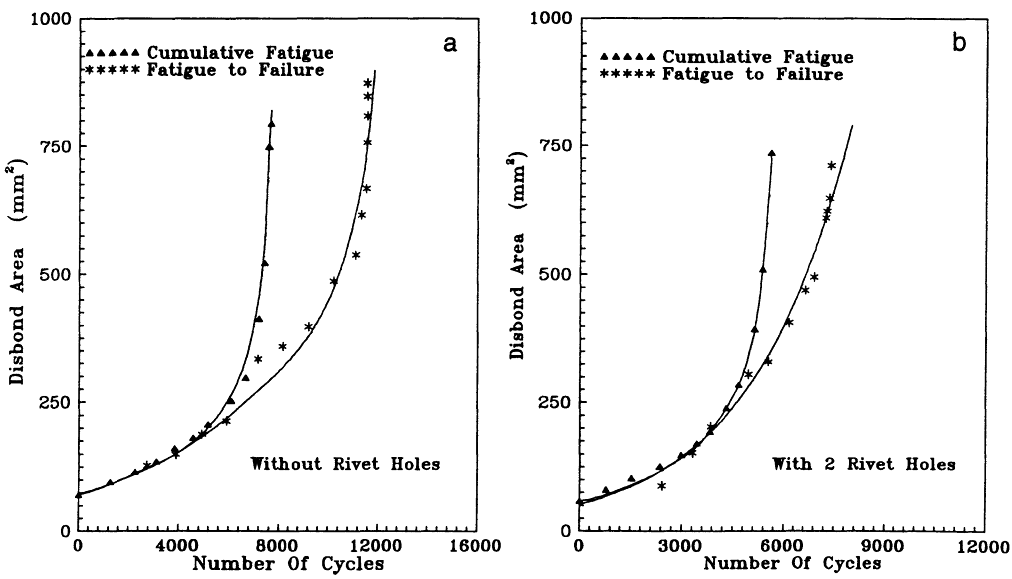

Figure 3 a and b. Comparison of the disbond propagation kinetics of specimens fatigued to failure and failed by cumulative fatigue.

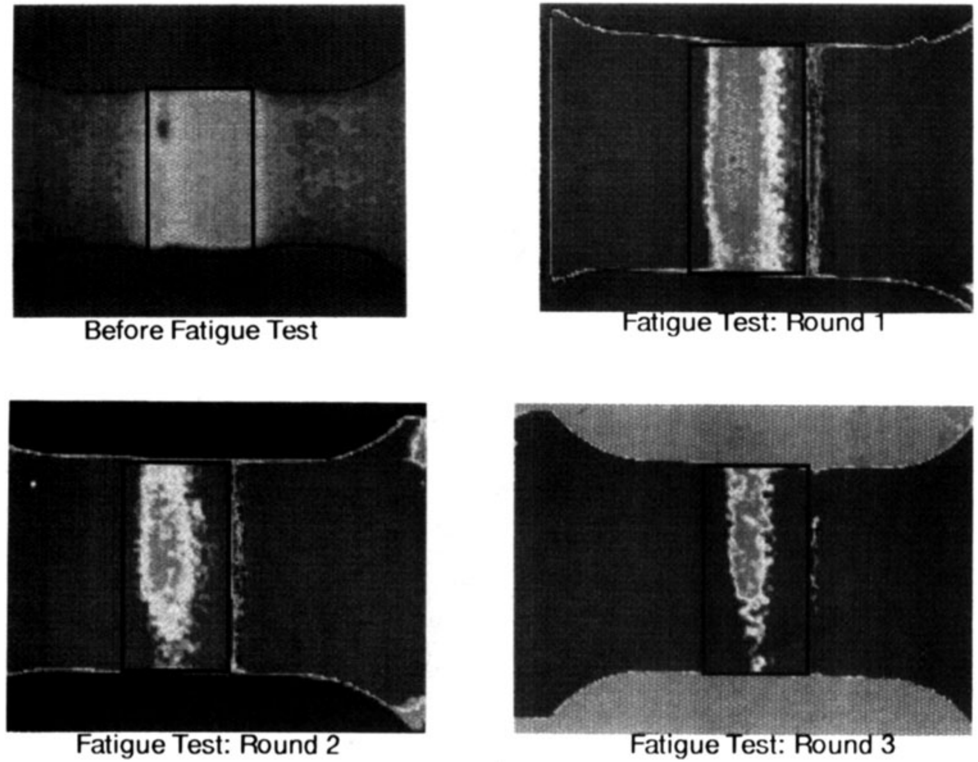

Figure 4. Thermal wave images of cumulative fatigue disbonds in adhesive joints without rivet holes. The black rectangles represent adhesive region and light area inside indicates the bonded regions while the dark areas indicate disbonds.

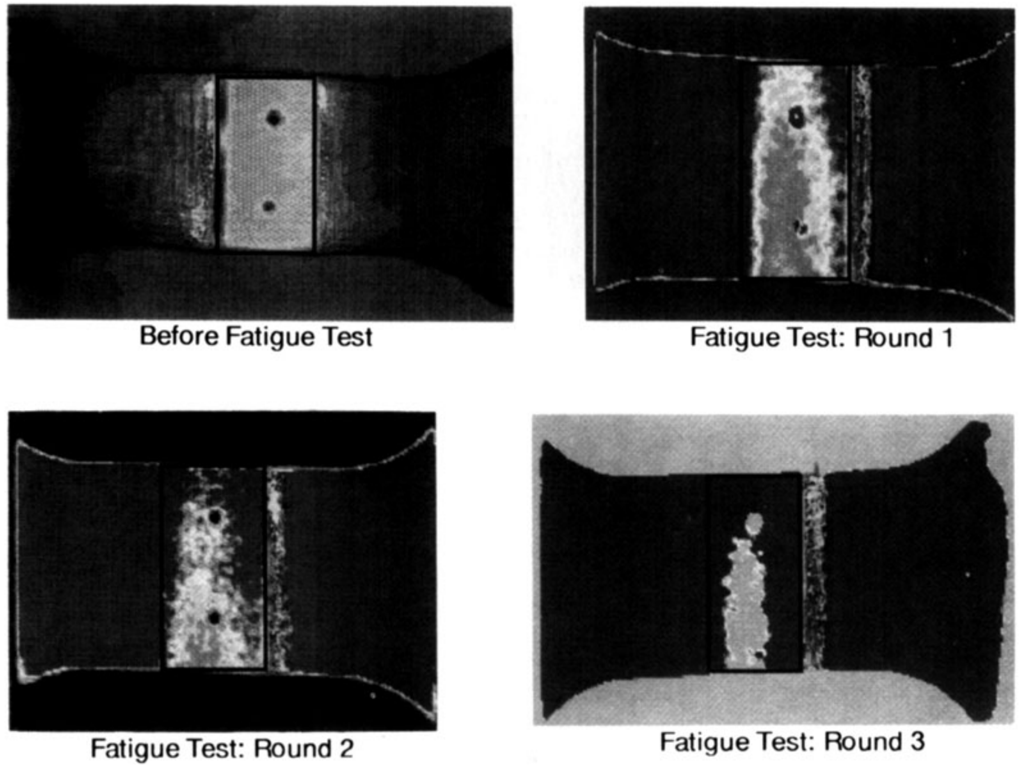

Figure 5. Thermal wave images of cumulative fatigue disbonds in adhesive joints with rivet holes. The black rectangles represent adhesive region and light area inside indicates the bonded regions while the dark areas indicate disbonds.

Figures 4 and 5 show the thermal images of disbond area for the cumulative fatigue tested specimens without and with rivet holes respectively, taken after every round of testing. The disbonded area is shown in black, the bonded area in grey and the light shaded area probably represents the damaged zone, ahead of the disbonded area (crack). From these figures it is clear that, thermal imaging can easily distinguish between the bonded and disbonded areas and it could be used to monitor disbond propagation in adhesively bonded joints. Also, this figure supports the prevailing view [15], that in adhesive lap joints most of the load is being carried by the outer circumferential area and the role of the central region comes at later stages prior to catastrophic (cohesive) failure of the joints. The assumption made initially regarding a trapezoid shaped disbond is found to be reasonable as seen from Figures 4 and 5.

Comparison between microscopic observations and thermal wave imaging of cumulatively tested specimens is shown in Figures 6 a and b. Initially, the two methods of disbond measurement differ and the difference between the microscopic and thermal wave imaging results decrease with the progress of disbond. This earlier difference in the two methods can be attributed to the following factors. First, visual methods can only detect the interfacial disbond (complete separation between the adhesive and the adherend) while, monitoring the damaged zone ahead of the disbond front is possible with the aid of thermal imaging. Secondly, due to the delay in thermal measurements from the time of fatigue testing, the seepage of air and moisture into the interfacial layer could degrade the joint.

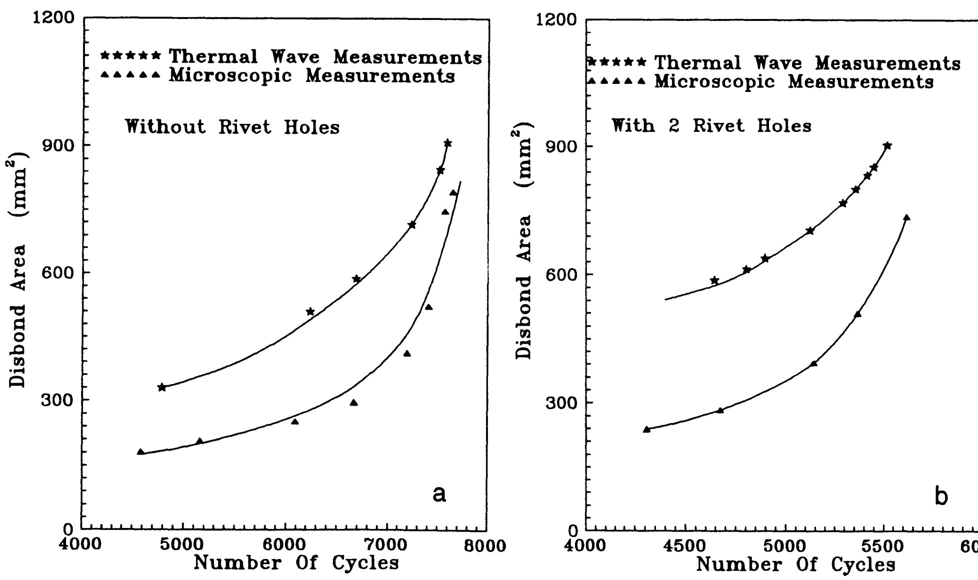

Figure 6 a and b. Comparison of thermal wave and microscopic disbond area measurements.

CONCLUSIONS

A cumulative fatigue cycling program has been carried out to investigate its affect on the lifetime of adhesive joints. This was performed on aluminum substrates bonded with 3M structural adhesive, without and with rivet holes. The data obtained from cumulative cycling were compared to data previously obtained from joints cycled to failure. A decrease of nearly 33% and 24% in lifetime is observed in the joints, without and with rivet holes respectively, failed by cumulative testing. The results also indicate that, thermal wave imaging is capable of detecting disbonds in all the stages of cycling. The discrepancy between the microscopic and thermal wave disbond detection becomes less with increasing rounds of cycling.

ACKNOWLEDGEMENTS

This work is sponsored by the FAA-Center for Aviation Systems Reliability, operated by the Ames Laboratory. USDOE, for the Federal Aviation Administration Technical Center at Atlantic City, New Jersey, under contract No.W-7405-ENG-82 with Iowa State University. The authors are grateful to the 3M company for providing the scrim cloth structural adhesive. The support of Dave Galella, the FAA technical monitor is acknowledged.

REFERENCES

1. F.H. Chang et al., IEEE Trans. Sonics Ultrason, SU-23(5), (1976), p. 334.
2. G.A. Alers et al., Materials Evaluation, 35(4), p. 77, (1977).
3. P.B. Nagy and L. Adler, J. Appl. Phys., 66 (10),(1989) p.4658.
4. Y. Bar-cohen and A.K. Mal, in Review of Progress in QNDE, Vol. 9, eds. D.O. Thompson and D.E. Chimenti (Plenum, New York, 1990), p. 1271.
5. P. Cawley and M.J. Hodson, in Review of progress in QNDE, Vol. 8, eds. D.O. Thompson and D.E. Chimenti (Plenum, New York, 1989), p. 1377.
6. S.I. Rokhlin, in Adhesive Joint, Formation, Characterization, and Testing, ed. K.L. Mittal (Plenum, New York, 1982), p. 307.
7. R.B. Thompson and D.O. Thompson, J. Adhesion Sci. Tech. 5, p. 583, (1991).
8. G.M. Light and H. Kwun, SwRI Project 17-7958-838, Southwest Research Institute, San Antonio, TX, (June 1989).
9. W.J. Xu et al., in Review of progress in QNDE, Vol. 13, eds. D.O. Thompson and D.E. Chimenti (Plenum, New York, 1994), p. 1499.
10. D.C. Worlton, J. Appl. Phys., 32, 967, (1961).
11. H. Aglan et al., in Review of progress in QNDE, Vol. 13, eds. D.O. Thompson and D.E. Chimenti (Plenum, New York, 1994), p. 1563.
12. P. Cawley and T. Pialucha, in Review of progress in QNDE, Vol. 13, eds. D.O. Thompson and D.E. Chimenti (Plenum, New York, 1994), p. 1523.
13. L. Molent and R. Jones, Eng. Fract. Mech., 44, 4, p. 627, (1993).
14. L.D. Favro, T. Ahmed, X. Wang, Y.X. Wang, H.J. Jin, P.K. Kuo and R.L. Thomas, in Review of Progress in QNDE, Vol. 12, eds. D.O. Thompson and D.E. Chimenti (Plenum, New York, 1993), pp. 2021-2025.
15. H. Aglan et al., J. of Adhesion Sci. and Tech., in press.